HHS Public Access

Author manuscript

Mol Neurobiol. Author manuscript; available in PMC 2016 July 01.

Published in final edited form as:

Mol Neurobiol. 2016 July ; 53(5): 3235–3248. doi:10.1007/s12035-015-9223-1.

A single injection of recombinant adeno-associated virus into the lumbar cistern delivers transgene expression throughout the whole spinal cord

Yansu Guo[1,2], **Dan Wang**[3], **Tao Qiao**[2], **Chunxing Yang**[2], **Qin Su**[3,4], **Guangping Gao**[3,5,*], and **Zuoshang Xu**[2,6,7,*]

[1]Department of Neurology, the Second Hospital of Hebei Medical University, 215 Heping West Road, Shijiazhuang, Hebei 050000, China

[2]Department of Biochemistry and Molecular Pharmacology, University of Massachusetts Medical School Worcester, Massachusetts 01605, USA

[3]Gene Therapy Center, University of Massachusetts Medical School Worcester, Massachusetts 01605, USA

[4]Viral Vector Core, University of Massachusetts Medical School Worcester, Massachusetts 01605, USA

[5]Microbiology and Physiology Systems, University of Massachusetts Medical School Worcester, Massachusetts 01605, USA

[6]Department of Cell Biology, University of Massachusetts Medical School Worcester, Massachusetts 01605, USA

[7]Neuroscience Program, University of Massachusetts Medical School Worcester, Massachusetts 01605, USA

Abstract

The lack of methods to deliver transgene expression in spinal cord has hampered investigation of gene function and therapeutic targets for spinal cord diseases. Here we report that a single intrathecal injection of recombinant adeno-associated virus rhesus-10 (rAAVrh10) into the lumbar cistern led to transgene expression in sixty to ninety percent of the cells in the spinal cord. The transgene was expressed in all cell types, including neurons, glia, ependymal cells and endothelial cells. Additionally, the transgene was expressed in some brain areas up to the frontal cortex and the olfactory bulb. The rAAV was distributed predominantly in the spinal cord, where its genome copy was over ten times that of the peripheral organs. Compared with intravenous injection, another method for rAAV delivery to the broad CNS, the intrathecal injection reduced the dosage of rAAV required to achieve similar or higher levels of transgene expression in the CNS by ∼100

*Co-corresponding author: Zuoshang Xu, Department of Biochemistry and Molecular Pharmacology, University of Massachusetts Medical School Worcester, Massachusetts 01605, USA, zuoshang.xu@umassmed.edu or Guangping Gao, Gene Therapy Center, University of Massachusetts Medical School Worcester, Massachusetts 01605, USA, guangping.gao@umassmed.edu.

Competing interests: G. Gao is a founder of Voyager Therapeutics and holds equity in the company. G. Gao is an inventor on patents on many rAAV serotypes including rAAVrh10 with potential royalties licensed to Voyager Therapeutics and other biopharmaceutical companies.

fold. Finally, the transduced areas were colocalized with the perivascular spaces of Virchow-Robin, from which the rAAV spreads further into the CNS parenchyma, thus suggesting that rAAV penetrated the CNS parenchyma through this pathway. Taken together, we have defined a fast and efficient method to deliver widespread transgene expression in mature spinal cord in mice. This method can be applied to stably overexpress or silence gene expression in the spinal cord to investigate gene functions in mammalian CNS. Additionally, this method can be applied to validate therapeutic targets for spinal cord diseases.

Keywords

rAAV; AAV; amyotrophic lateral sclerosis; pain; SMA; gene therapy

Introduction

Efficient and sustained expression or suppression of the gene of interest *in vivo* is a powerful tool for investigating gene function in mammalian tissues including the central nervous system (CNS). Currently this is mostly achieved through genome modification in mice (e.g. transgenic mice with random transgene insertion or targeted gene knockin or knockout). However, these processes are extremely time-consuming and expensive. For selective transgene expression in mature adult CNS, construction of transgenic mice with conditional transgene expression is necessary. This process requires construction of multiple transgenic lines and intercrossing them to obtain desired genotype [1], thus further exacerbating the problem of long experiment time and high cost.

To circumvent this problem, recombinant viral vectors are often used to deliver transgene expression. Recombinant adeno-associated viruses (rAAVs) are increasingly becoming the vector system of choice for gene expression *in vivo* because of its broad cell and tissue tropism, efficient gene transfer, long-lasting transgene expression, minimal immunogenicity and toxicity [2]. For application in the CNS the vector is commonly stereotactically injected into the parenchyma or ventricles, leading to transgene expression in the vicinity of the injected areas. While this is well suited for investigating gene function in compact areas of the brain, such as the amygdala, nucleus accumbens or substantia nigra, it is difficult to investigate gene function in the spinal cord due to its long linear structure.

Recent evidence has shown that intrathecal injection into the CSF in lumbar cistern may be advantageous in delivering transgene expression to the spinal cord. According to the classical model of CSF circulation, the CSF is secreted from the choroid plexus in the ventricles, flows through the ventricles and exits into the cistern magnum through the median and lateral apertures of the fourth ventricle. It then circulates through the subarachnoid space around the spinal cord and upward to the arachnoid granulation, where it is absorbed into the superior sagittal sinus and returns into the blood stream. Based on this knowledge, the rAAVs injected into the lumbar cistern should follow CSF flow through the entire length of the spinal cord and possibly further to the forebrain. Numerous studies have tested this idea and the widest distribution of gene transduction was achieved compared with

other approaches [3-10]. Several studies showed strong gene transduction along the entire length of the spinal cord following a single injection into the CSF [8-10].

Despite these advances, further understanding and improvement of this approach are needed for its wide use in studies of gene function in spinal cord. For example, it is not yet clear whether there are advantages in using intrathecal injections over intravenous injections. The relative extent of CNS and peripheral transduction following intrathecal delivery of rAAV remains unknown. Current delivery methods in small animals such as mice include lumbar laminectomy and intrathecal catheterization, which are tedious, invasive and injurious, resulting in highly variable and unpredicatable transduction outcomes [8]. Furthermore, how the rAAV injected into the CSF spreads into the CNS parenchyma remains a mystery. To address these questions, we conducted a systematic study on the biodistribution of rAAVrh10 following a single intrathecal injection by lumbar puncture in mice. Although lumbar puncture in mice is technically more challenging than in larger animals, we chose this species because mice are most used to construct genetic models for human diseases. Therefore, technical optimizations in rAAV delivery can be directly applied in testing hypotheses on disease mechanism and therapy.

In this study, we injected the rAAV into the lumbar cistern and showed that a single injection consistently led to robust transduction of neurons, glia, ependymal cells and endothelial cells along the entire length of the spinal cord and that transduction spread as far as the forebrain and olfactory bulb. We compared transduction patterns between mice that were injected intrathecally with those that were injected intravenously. We found that the intrathecal injections produced ten times higher rAAV biodistribution in spinal cord than in peripheral organs, whereas intravenous injections produced the opposite rAAV biodistribution pattern. Intrathecal injections yielded higher CNS rAAV biodistribution even with a dose ∼100 times lower than intravenous injections. Moreover, we analyzed the spatial pattern of the rAAV gene transduction and found that the pattern was colocalized with the perivascular space of Virchow-Robin. These results suggest that rAAV injected into the CSF spread into the CNS parenchyma through this channel. Based on these findings, we conclude that intrathecal injection of rAAVrh10 is a simple and fast method to deliver broad transgene expression throughout the spinal cord. By incorporating overexpression or knockdown constructs, this rAAVrh10 delivery method can be a highly efficient tool for investigation of gene functions in the spinal cord.

Material and Methods

rAAV vector and delivery

The gene cassette expressing EGFP and a scrambled artificial miRNA (amiR-Scr) is driven by cytomegalovirus enhancer/chicken β-actin promoter. The amiR-Scr is placed in an intron located in the 3′ untranslated region (UTR). This self-complementary rAAV construct was built, produced, and used as described previously [8,11]. FVB/NJ mice were purchased from the Jackson Laboratory and bred in the animal facility of the University of Massachusetts Medical School. The mice aged 30-70 days were used in the experiments. All mouse experiments were approved by IACUC and conducted according to UMMS policies and

procedures regulating the use of animals in research and the provisions of the PHS/NIH Guide for the Care and Use of Laboratory Animals.

Direct lumbar puncture [12] was used to deliver the rAAV vector. The injection was conducted in awake, conscious mice using the following procedure: A soft cloth was placed over the head and upper body of the animal to keep it calm. The animal was gripped firmly, but gently, by the pelvic girdle. The skin above the ileac crest was shaved and cleaned with alcohol. A 27-gauge needle connected to a 50-μl Hamilton syringe was inserted at the midline directly between the vertebrae at the level of the cauda equina. Once we observed the reflexive tail flick that is indicative of puncture of dura, eight microliters of PBS containing 4×10^{10} rAAV and 1% lidocaine hydrochloride (Sigma) was injected. After injection, the needle was maintained in place for ∼1 min before withdrawal and the animal was released in its cage. A transient weakness of the mouse limbs was monitored to assess the degree to which the injection reached the CSF: score 0 indicated no weakness, score 1 minor weakness of hind limbs without obvious gait abnormality, score 2 moderate weakness of hind limbs with gait abnormality, score 3 paralysis of hind limbs, score 4 paralysis of hind limbs and moderate weakness of fore limbs, score 5 paralysis of all four limbs. The injected mice were maintained for 3 weeks and sacrificed for evaluation of transduction efficiency, which was then correlated with the original weakness score in the individual animals.

Histological processing, immunostaining and quantitative analysis

Mice were deeply anesthetized at 21 days post-injection and transcardially perfused with ice-chilled PBS followed by cold fixation buffer containing 4% paraformaldehyde in PBS. Brain and spinal cord were dissected and post-fixed by soaking in the same fixative for 48 h. Tissues were cryoprotected in 30% sucrose for 24-48 h and then embedded in OCT compound. Twenty micron frozen sections were cut using a Thermo cryostat.

For immunofluorescence staining, free-floating sections of brain and spinal cord or whole mount of ventral, dorsal roots and dorsal root ganglia (DRG) were incubated in 1% Triton X-100 in PBS for 30 min, washed with PBS for 2 min and then incubated in blocking solution containing 10% serum, 0.05% Triton X-100 and 0.05% Tween 20 in PBS for 30 min at room temperature. Primary antibodies in the blocking solution were added to the sections or roots and incubated at 4°C overnight. The primary antibodies and dilutions used were as follows: rabbit anti-GFP (Invitrogen G10362, 1: 330) was used with mouse anti-NeuN (Millipore MAB377, 1:100), GFAP (Cell Signaling #3670S, 1:500) or APC (EMD Bioscience OP80-100UG, 1:400); mouse anti-GFP (Life Technologies, A11120, 1:330) was used with rabbit anti-Iba1 (BioCare Medical CP290A, B, 1:500), AQP4 (Alomone lab AQP-004, 1:200) or CD31 (Bioss bs-0468R, 1:300). Following the incubation, sections or roots were washed in PBS three times for 5 min each, incubated in the appropriate secondary antibody at room temperature for 90 min, washed three times for 5 min each, mounted with VECTASHIELD mounting solution and sealed with nail polish. Images of the brain, spinal cord sections and roots were taken with a Leica TCS SP2 Confocal Microscope.

For Immunohistochemistry, free-floating sections of brain and spinal cord were pre-treated with 1% H_2O_2 for 10min and then washed three times in PBS. After incubation with

blocking solution containing 5% normal serum and 0.3% Triton X-100 in PBS, primary antibodies in the blocking solution were added to the sections and incubated at 4°C overnight. Following incubation, sections were washed three times in PBS containing 0.25% Tween 20 (PBST) for 5 min each, and then incubated in appropriate biotin-secondary antibody at room temperature for 120 min. Sections were then washed three times in PBST, stained following the manufacturer's instructions for VECTASTAIN ABC kit and Elite PK-6100 standard ImmPact tm DAB peroxidase Substrate kit SK-4105 (Vector Lab). The sections were then mounted on slides and dried. After soaking in Xylene two times for 2 min each, the slides were sealed with Permount (Vector Lab) and photographed with Olympus CX41 microscope equipped with an Evolution MP 5.0 RTV CCD (Color-Media Cybernetics, Canada).

Staining intensities in the digital images of transverse spinal cord sections were measured in grayscale using Image-pro plus 6.0 software. For analysis of EGFP positive cells, photographs made with 40× objectives were used to count the total number of GFP-positive cells manually. Briefly, three different lumbar and cervical sections from each well-injected mouse (scored at 4-5) were stained for EGFP, counterstained with Haematoxylin and analyzed. All cells with a clearly visible nucleus in one 40× field (72-194 cells) per section were counted. Cells with dark brown staining were classified as GFP-positive, cells with light-brown staining as possible GFP-positive and cells without brown staining as GFP-negative. The percentage of GFP-positive, probable GFP-positive and negative cells in each region were recorded.

rAAV genome copy number and RNA quantification

Tissues were quickly harvested, snap frozen in liquid nitrogen and stored at -80°C. Total DNA or RNA from ∼10-20 mg of tissue blocks was extracted using the QiaCube HT instrument and reagent kits (Qiagen) according to the manufacture's protocols. Total DNA was extracted using the QIAamp 96 DNA QIAcube HT kit (Qiagen, 51331), and digested with EcoRI (NEB) at >10 U/ug of DNA under 37°C for 1 hour. There are two EcoRI sites in the rAAV genome. The EcoRI digestion ensures single copies of EGFP transgene for droplet digital PCR (ddPCR) quantification. Multiplexed ddPCR was performed on a QX200 ddPCR system (Bio-rad) using Taqman reagents targeting EGFP (Invitrogen, Assay ID Mr00660654_cn) and the reference gene transferrin receptor (Tfrc) (Invitrogen, 4458367). rAAV genome copy numbers per diploid genome were calculated as EGFP transgene copy numbers per two Tfrc gene copies. Total RNA was extracted using the RNeasy 96 QIAcube HT kit with on-column DNase I digestion (Qiagen, 74171). Approximately 1.5 ug of total RNA was reverse transcribed into cDNA (Invitrogen 4368813), and subjected to multiplexed ddPCR using Taqman reagents targeting EGFP (Invitrogen, Assay ID Mr00660654_cn) and beta glucuronidase (GUSB) (Invitrogen, Assay ID Mm01197698_m1). The quantity of EGFP mRNA was normalized to GUSB mRNA, and expressed as EGFP mRNA copy numbers per GUSB mRNA copy.

Western Blot

Total protein was extracted from frozen tissue by homogenization in a solution containing 1% SDS, 25 mM phosphate (pH 7.6), 1mM EGTA and Halt Protease Inhibitor Cocktails

(Thermo Scientific). The protein concentration was determined by BCA assay (Pierce) according to the manufacturer's protocol. To detect GFP protein, 30 μg of total protein was separated on a 15% SDS-polyacrylamide gel (Bio-Rad) and wet transferred to a Protran ® (Whatman GmbH) nitrocellulose transfer membrane. The membrane was probed with rabbit anti-GFP antibody (Cell Signaling 2555S) and donkey anti-rabbit IgG (Amersham ECL NA34) secondary antibody. The protein bands were visualized using SuperSignal West Pico kit (Pierce).

Results

rAAVrh10 transduces full length of the spinal cord following injection into the lumbar cistern

To find an efficient method to deliver rAAVrh10 to the spinal cord, we tested the lumbar puncture method in mice. To gauge how rAAV spreads after injection, we first tested using Trypan blue. To monitor the quality of each injection, we added 1% lidocaine hydrochloride to the injection solution. Well-injected animals where the injection went into the subarachnoid space were expected to show transient paralysis of the limbs whereas poorly injected animals would show no or mild weakness. As expected, mice showed various degrees of transient weakness or paralysis for 2-4 min and then resumed normal activity. We established a semi-quantitative five-point scoring system for the various degrees of transient limb weakness (see Methods). In well-injected animals that scored four or five, the dye spread throughout the entire spinal cord and up to the furthest CNS areas such as the olfactory bulb within 10 minutes after injection (Figure S1). Thus, the solutes injected into the CSF by lumbar puncture can spread rapidly throughout the CNS.

Next we injected rAAVrh10-EGFP and tested whether we could use the five-point scoring system for the various degrees of lidocaine-induced limb weakness immediately after injection to predict the extent of rAAV gene transduction that would be evaluated three weeks later. Of the ten mice injected, two showed no weakness (score 0), one showed minor weakness of hind limbs (score 1), four showed paralysis of hind limbs and moderate weakness of fore limbs (score 4), three showed paralysis of four limbs (score 5) (Figure S1). These mice were evaluated for their transduction levels by EGFP immunostaining of the spinal cord. The zero-scored mice manifested either no transduction or some transduction in the grey matter and in areas where nerve roots exit or enter the spinal cord (Fig. 1A); the one-scored mouse was similar to the zero-scored mice but had a slightly increased transduction (Fig. 1A); the four and five-scored mice showed strong and global transduction in the whole spinal cord with the highest transduction in the nerve root entry or exit zones and patches of strong transduction in the white matter (Fig. 1A). We quantified the GFP staining intensity, which showed a positive correlation with the extent of transient limb weakness in individual mice (Fig. 1B). Therefore, we concluded that the severity of paralysis can be used to assess the quality of injection and predict the extent of transduction.

We further examined the spinal cord transduction in well-injected mice and noticed that the full length of the spinal cord was well transduced (Fig. 2). Particularly notable were the strong GFP-positive areas including the ventral and dorsal horns, the ventral effluent motor axons and dorsal affluent sensory axons (Fig. 2, areas A, B, D, G, H, I, J and L). In the

spinal cord, motor neurons at all levels were robustly transduced (Fig. 2, areas A, G and I). Moreover, the grey matter areas strongly expressed GFP and white matter areas contained slightly less GFP –positive cells. However, a quantitative assessment of transduced cells showed a similarly high percentage of transduced cells in both areas (Fig. 3), thus indicating that the relatively weaker staining in the white matter reflected a relatively lower cell density compared with the grey matter. Overall, between sixty and ninety percent of the cells in the spinal cord were GFP-positive (Fig. 3).

To confirm the cell types that were transduced, we carried out double immunofluorescence staining. We detected GFP expression in motor neurons and glial cells such as astrocytes, oligodendrocytes and microglia (Fig. 4). Additionally we found robust GFP expression in DRG neurons as well as Schwann cells in ventral and dorsal roots (Figure S2), thus indicating that intimate exposure to the CSF provides easy access to the rAAV.

rAAVrh10 transduces cells in areas near the surface of brainstem but broadly in cerebellum

To examine whether rAAVrh10 could spread beyond the spinal cord, we investigated transduction patterns in brainstem and cerebellum from well-injected mice. Generally, the brainstem and cerebellum were widely transduced (Figures S3-S6). In the lower medulla, transduction was detected in both deep and superficial areas with the latter showing stronger transduction (Figure S3). In the rostral medulla (Figure S4) and pons (Figure S5) the superficial areas were strongly transduced and few cells were observed in the deep areas. Similarly, we observed strong and weak transduction in superficial and deep areas, respectively in the midbrain (Figure S6). Thus, the pattern of transduction in brainstem indicates that the exposure and distance to the CSF determined efficiency of rAAVrh10 transduction.

Despite weak transduction in the deep regions of the rostral brainstem, many of the brainstem nuclei were robustly transduced, including the oculomotor nucleus (Figure S6, area A), trigeminal nucleus, facial nucleus (Figure S5, area A), vestibular nucleus (Figures S4, areas B and C, S5, areas F and G), motor nucleus of vagus (Figure S3, area A), hypoglossal nucleus (Figure S3, area B), cuneate nucleus (Figure S3, area E), prepositus nucleus (Figures S4, area D, S5, area H), reticular nucleus (Figures S3, areas C and H, S4, area I, S5, area C) and substantia nigra (Fig. 5, area C, Figure S6, areas G, I, and J). Among the cells transduced in the brainstem nuclei, both neurons and glial cell were GFP-positive. In addition, robust GFP signals were detected in axon tracks, including inferior cerebellar peduncle (Figures S3, area G, S4, area E), spinal trigeminal tract (Figures S3, area G, S4, area F, S5, area E) and solitary tract (Figure S4, area A), suggesting that neurons from which these fibers originate were transduced. Pyramidal tracts expressed EGFP but the signal was not as strong as the other tracks (Figures S3-S5). Many glial cells were transduced in or near the pyramidal tract (Figures S3, area D, S4, area H, S5, area B).

The cerebellum was widely and strongly transduced, including Purkinje cells, granule cells, cells and axons in the white matter and deep cerebellar nuclei (Figure S5).

rAAVrh10 transduces cells in the surface and deep regions of the forebrain

Similar to the brainstem, areas close to the CSF in the subarachnoid space were well transduced, including the cortex, hippocampus and olfactory bulb (Fig. 5; Figures S7, S8). Caudal coronal forebrain section containing midbrain and hippocampus showed readily detectable transduction of parietal and temporal cortices. The transduced cells were distributed along the surface of the cortex in patches, which extend from the surface into deep layers of the cortex, reaching layer VI in many areas (Fig. 5, arrows in the center panel). Within these cortical patches, most EGFP-positive cells were neurons with well-marked apical dendrites (Fig. 5, areas J, M and N). However, some scattered or clustered GFP-positive glial cells can also be detected (Fig. 5, areas M, N and R). In addition, the hippocampus was differentially transduced with EGFP-positive neurons scattered in the dentate gyrus (Fig. 5, area K). Numerous EGFP-expressing cross-sectioned fibers and interneurons were found in the polymorphic layer of dentate gyrus (Fig. 5, area O). Furthermore, many EGFP-positive fibers were also observed in the inner third of the molecular layer of dentate gyrus (Fig. 5, area P). CA3 of the hippocampus was highly transduced, including pyramidal, molecular, and oriens layers (Fig. 5, areas L and Q). Neurons in CA1 of hippocampus were lightly transduced, while fibers in oriens and radiatum layers were moderately transduced (not shown). In contrast, the midbrain covered by the forebrain (Fig. 5, areas A-H) was relatively less transduced compared with its caudal part that was exposed to the CSF (Figure S6). Marginal areas including medial mammillary nucleus (Fig. 5, area A), rostral interpeduncular nucleus (Fig. 5, area B), posterior intralamina thalamic nucleus (Fig. 5, area F), medial genic nucleus (Fig. 5, area G), superior colliculus (Fig. 5, area I) were strongly transduced. Substantia nigra (Fig. 5, area C) and parabrachial pigmented nucleus (Fig. 5, area D) were moderately transduced, while only a few cells were transduced in the deep areas (Fig. 5, areas E and H). Generally, GFP-positive cells in the deep areas away from the CSF were mostly astrocytes with abundant ramifications (Fig. 5, area E).

Rostral coronal brain sections generally displayed a similar transduction pattern. The external cortex areas of each semisphere such as the cingulate cortex and indusium griseum near the median fissure were strongly transduced, while deep thalamus areas were poorly transduced (Figure S7, areas A and B). Most of the cortex was highly transduced, with noticeably higher EGFP-positive neurons and glial cells observed among all the cortical layers (Figure S7). Deep areas showed low transduction with a few clusters of glial cells and evenly distributed fibers in the corpus callosum (Figure S7, area D). Sparse EGFP-positive neurons and glial cells were observed in the caudate putamen (Figure S7, area G); however, midline areas that included dorsal peduncular cortex (Figure S7, area E) and medial septal nucleus (Figure S7, area H) were transduced. Meanwhile, fibers and a few glial cells were transduced in the anterior commissure (Figure S7, area J). A number of glial cells were EGFP positive in the core nucleus accumbens (Figure S7, area K). Moreover, ventral pallidum (Figure S7, area I) and nucleus of vert limb diagonal band (Figure S7, area L) were prominently transduced. The most rostral part of the mouse brain where the olfactory bulb is located also showed a clustered transduction pattern (Figure S8) of EGFP positive neurons (Figure S8, areas A, B and D) and glial cells (Figure S8, area C) in the periphery and center of the olfactory bulb.

Similar to the spinal cord (Fig. 4), double immunofluorescence staining confirmed that all the major CNS cell types, including neurons, astrocytes, oligodendrocytes and microglia were transduced in the brain (Figure S9).

Injection of rAAVrh10 by lumbar puncture causes no detectable neuroinflammation

CNS neuronal damage caused by immune responses to viral gene transfer had been reported in rAAV-mediated transductions [13,14]. Likewise, we also observed astrogliosis and microgliosis after intrathecal delivery of rAAVrh10 through a catheter implanted by laminectomy [8] (data not shown), suggesting a presence of injury using that approach. To determine whether rAAVrh10 delivery by lumbar puncture caused similar injury, we examined gliosis in the robustly transduced areas such as the lumbar and cervical regions of the spinal cord as well as the cerebral cortex. No astrogliosis, microgliosis or neuronal loss was detected, (Figure S10), suggesting that intrathecal injection of rAAVrh10 into the CSF by lumbar puncture can avoid injuries associated with laminectomy and intrathecal catheterization.

rAAVrh10 penetrates the CNS parenchyma through perivascular spaces of Virchow-Robin

The spread of the CSF-injected rAAV and its transduction of cells deep in the CNS parenchyma raised the question as to how viral particles penetrate into the CNS tissue. In the spinal cord and brain sections, we noticed that rAAV transduction was often distributed along imaginative lines penetrating the deep CNS parenchyma from the surface (Fig. 6, arrows in the panels in the center of Figs. 2, 5, Figures S4, S5). This pattern was similar to that observed when macromolecular tracers were injected into the CSF, demonstrating that these tracers reached the CNS parenchyma through the perivascular spaces of Virchow-Robin [15,16]. Therefore, we postulated that rAAV particles injected into the CSF penetrate and spread into the CNS parenchyma through the same route. To test this, we conducted double immunofluorescence staining of EGFP and aquaporin 4 (AQP4), a marker enriched in the astrocytic end feet aligning the perivascular space. The center of the EGFP-stained patches was colocalized with the AQP4-positive perivascular channels in the cortex. From these channels the EGFP signal spread laterally (Fig. 7A). Furthermore, a similar colocalization pattern was observed in the spinal cord (Fig. 7A). Lastly, we also observed strong transduction in endothelial cells (Fig. 7B). These results suggest that rAAVs gain access to the CNS parenchyma through the perivascular channels.

Intrathecal injection of rAAVrh10 by lumbar puncture enhances the CNS gene transduction

Although intrathecal injections of rAAV have been used in several previous studies, a systematic study on the transduction levels in various regions of the CNS relative to the periphery has not been conducted. To fill this gap, we measured rAAV genome copies for the rAAV distribution, and measured EGFP mRNA and protein levels for the transgene expression in well injected animals with weakness scores of 4 and 5 (Fig. 1). The results revealed four patterns (Fig. 8). First, with an exception to the cerebellum, genome copies of rAAV were generally higher in the CNS than in the periphery (Fig. 8A, black bars). Notably, our results show that of all the CNS regions, the lumbar spinal cord showed ten times more genome copies than the most transduced peripheral organ, the adrenal gland (Fig. 8A, black bars). Second, within the CNS, regions near the injection site generally had higher rAAV

genome copies than the more distal regions (Fig. 8A, black bars) with the exception of cerebellum, which showed exceedingly low biodistribution (Fig. 8A, black bars). Third, the levels of EGFP expression showed a gradient that ranged from high near the injection site to low at more distant sites. Fourth, when comparing the highest EGFP levels from both CNS and peripheral tissues, we observed more EGFP expression in the adrenal gland and heart than the lumbar spinal cord (Figs. 8B, C). Other peripheral organs such as the liver and skeletal muscle also expressed EGFP levels higher than most CNS regions. Taken together, the transgene expression did not follow the pattern of rAAV distribution. Indeed, when normalized against the genome copy, several peripheral tissues (heart, adrenal gland, muscle and liver) showed higher transgene expression efficiency (TGEE) than the CNS tissues with the exception of cerebellum, which showed a level of TGEE comparable to the highest peripheral tissue (Fig. 8D).

The relative transduction levels in the CNS and the periphery might be determined by the injection quality. For example, in our previous study where the animals were injected by laminectomy and intrathecal catheterization method, only the well-injected animals showed relatively higher CNS transduction than the periphery. On the other hand, poorly injected animals showed relatively higher peripheral transduction than the CNS because most of the rAAV may have leaked to the periphery during injection [8]. To examine this in animals injected by lumbar puncture method, we investigated the rAAV biodistribution and EGFP expression in poorly injected animals with low weakness score (Fig. 1). Our results showed that poorly injected animals had lower transduction levels in both the CNS and peripheral tissues than well-injected animals (Figs. 8A, B; comparing white bars with the black ones), but the relative ranking of transduction in various CNS regions and peripheral organs remained largely the same between the well and poorly injected animals (Figs. 8A, B; comparing the white bars or the blank bars among themselves). At the protein level, the intensity of EGFP expression is also correlated with the injection quality score in both the CNS and the periphery. Animals with a high injection quality score showed stronger transduction in both the CNS (Fig. 1) and the periphery than those with a low injection score (Fig. 1, Figure S11).

The broad CNS transduction can also be achieved by intravenous administration of rAAV in adult animals [17,18,11,19]. However, the transduction efficiency has not been quantitatively compared side-by-side with the intrathecal delivery. To obtain this data, we compared the genome copies of rAAVrh10 in different organs between the levels achieved by the intrathecal injection and those achieved by intravenous injection that we reported previously [19]. The intrathecal injection delivered rAAV predominantly to the CNS (spinal cord and brain) whereas the intravenous injection delivered rAAV predominantly to the periphery (e.g. liver and muscle) (Fig. 8E). Notably, the intrathecal injection achieved higher levels of CNS transduction than the intravenous injection with doses that were two orders of magnitude lower ($\sim 10^{12}$ vg/kg vs. $\sim 10^{14}$ vg/kg).

Discussion

In this study, we characterized transduction patterns of rAAVrh10 in the CNS following its intrathecal injection into the lumbar cistern. We show that this method can deliver

widespread and robust transgene expression throughout the entire spinal cord (Fig. 2). Sixty to ninety percent of cells in the spinal cord, including neurons (motor neurons, sensory neurons and interneurons) and glia (astrocytes, oligodendrocytes and microglia) showed transgene expression (Figs. 3, 4, Figure S2). In addition, gene transduction had spread to many brain regions including the olfactory bulb, the most anterior region of the mouse brain (Fig. 5, Figures S3-S8). Similar to the spinal cord, rAAVrh10 transduced all major CNS cell types in the brain (Figure S9). These results achieved unprecedented viral vector mediated gene transduction in the spinal cord, thus providing a means to investigating gene functions in this region.

The rAAV distribution in the CNS following CSF injection in the lumbar cistern is largely consistent with CSF flow pattern, suggesting that dispersion of rAAV in the CNS is at least in part assisted by the CSF flow. However, this did not hold true for all cases as we observed higher viral genome copies in the olfactory bulb than the cortex, and higher in the hippocampus and cortex than in the cerebellum (Fig. 8A). In both cases the latter regions encounter the rAAV brought by the CSF flow ahead of the former regions. Deviations from the CSF flow suggest that other factors also contribute to rAAV biodistribution. One such factor may be the ratio of surface area to volume of a region. Therefore, a higher ratio or larger surface area exposes the region to more CSF containing the rAAVs. This could explain the higher viral genome copies in the olfactory bulb and hippocampus than in the cortex and the cerebellum, respectively. Another contributing factor could be regional differences in the rAAV tropism. For example the rAAVrh10 may have lower tropism for cells within the cerebellum than other parts of the brain, resulting in the lowest rAAV biodistribution within the cerebellar region among all CNS areas. Overall, our results suggest that the exposure and distance to the CSF and the injection site are important determinants for rAAV distribution levels in the CNS regions following rAAV injection into the CSF.

Despite the increasing literature on the delivery of rAAV to the CNS by injection into the CSF, how the rAAV penetrate into the CNS parenchyma was not known. We found that the most intensely transduced areas in the spinal cord and brain were co-localized with the perivascular space of Virchow-Robin and a transduction gradient that spreads from this channel to the neighboring CNS parenchyma (Figs. 6, 7A). These results suggest that rAAV delivered into the CSF gain access to the CNS parenchyma through this pathway. Previous reports have shown that macromolecular tracers penetrate into the brain parenchyma through the same channels, which support this scenario [16, 20]. If this pattern is confirmed in further studies in different mammalian species, the abundance and depth of the penetrating perivascular spaces may predict the degree of transduction in the CNS parenchyma following rAAV delivery via CSF.

Although the perivascular space is likely the predominant channel through which the rAAV spreads into the CNS parenchyma, other routes are likely to also contribute. For example, transduction was also strongly colocalized with the ventral root exit and dorsal root entry zones (Figs. 1, 2). Strong transduction in glial cells surrounding the ventral and dorsal root axons (Fig. 2, areas B, D, J and L, Fig. 3a) suggests that axon tracks also facilitate the rAAV distribution into the CNS parenchyma. In addition, GFP-positive cells (mostly astrocytes and

some isolated neurons) were also observed in areas that are deep and furthest from the CSF and apparently not associated with the penetrating perivascular spaces (e.g. Fig. 5E, H; Suppl. Fig. 3B, C; the center panel of Suppl. Fig. 4-6; Suppl. Fig. 7E, F, G, H, J, K). It is not clear how the rAAV reach these deep areas. However, a small fraction of rAAV might spread trans-synaptically via long projecting axons and/or enter the blood stream and recirculate to reach the deep CNS parenchyma.

Comparisons between rAAV distributions following intrathecal injection and intravenous injection demonstrate that intrathecal injection is more efficient in delivering rAAV into the CNS, particularly the spinal cord (Fig. 8E). Other studies have also concluded that CSF injection is more efficient in delivering rAAV into the CNS [9,10]. However, peripheral distribution of the rAAV was also readily detectable following intrathecal injection, albeit at lower levels (particularly in liver) than in the CNS (Fig. 8A). Similar peripheral distribution has also been detected in other studies where rAAV9 or rAAVrh10 was injected into the CSF [9,10]. In this study, we analyzed both well and poorly injected animals and found that the rAAV distribution in both the CNS and the periphery changed in concert with quality of injection. Well injected animals showed higher levels of rAAV distribution than poorly injected animals in both the CNS and periphery (Fig. 8A). This finding suggests that the peripheral distribution was not a result from leakage of viral particles during the injection; but rather, systematic factors caused rAAVs to be consistently distributed to the periphery. It has been reported previously that small and macro molecules injected into the CSF can lead to blood distribution rapidly [21-23]. It is possible that structural conduits, such as the CSF drainage to the lymphatics, permitted the rAAV in the CSF to flow into the blood circulation [24]. Alternatively, the rAAV might cross arachnoid villi into the blood stream [25]. The exact channel through which the rAAV is distributed to the periphery remains to be determined by further investigation.

Our measurements of rAAV genome copies and the expression levels in different regions of the CNS and peripheral tissues have provided the first glimpse into the relationship between the rAAV distribution and the levels of transgene expression following the intrathecal delivery. In the CNS, both genome copies and mRNA levels displayed a gradient from the highest near the injection site to the lowest at the distant sites (Figs. 8A, B). When the data was presented as the mRNA level per rAAV genome or transgene expression efficiency (TGEE), an opposite gradient emerged: the TGEE was positively correlated with the distance from the injection site (with the cerebellum being the exception) (Fig. 8D). For example, the olfactory bulb is the farthest CNS region from the injection site, yet it expressed EGFP mRNA per rAAV genome ∼4 times higher than the lumbar spinal cord, the region that was the closest to the injection site (Fig. 8D). The variation in the levels of the GUSB mRNA, which was used to normalize the EGFP mRNA level, ranged from the lowest in the lumbar spinal cord to the highest (by ∼65%) in the olfactory bulb, and therefore, is not the cause for the correlation between the expression efficiency and the distance from the injection site.

When we include the cerebellum and the peripheral tissues in the comparison, the phenomenon that the levels of rAAV distribution do not directly translate into the levels of transgene expression becomes more striking. For example, while the highest copies of rAAV

genome were detected in the spinal cord (Fig. 8A), the highest levels of EGFP mRNAs were found in the peripheral organs such as the adrenal gland and the heart (Figs. 8B, C). By measuring both the genome copy numbers and the transgene expression levels, we were able to determine the TGEE. For each rAAV vector, the TGEE may not be predicted because it can be influenced by multiple factors, including the types of viral capsid, the vector promoter, the method of delivery and the variables in the host tissues such as viral receptor, internalization, intracellular trafficking, uncoating and genome processing [26]. Additionally, differences in tissue- and cell-specific regulation of gene expression could also affect the activity of the vector promoter, the levels of translation and the stability of the transgene products (mRNA and protein). Given these considerations, selective spinal cord expression may be further enhanced by utilizing different serotype or CNS-specific vector promoters [27,28].

Conclusions

Administration of rAAV into the lumbar cistern is a highly efficient method to deliver widespread and robust transduction of rAAV in the spinal cord. Compared with intravenous injection, the intrathecal injection delivered more selective CNS transduction relative to the peripheral transduction. Additionally, the intrathecal injection delivered widespread rAAV transduction through the perivascular spaces in the CNS. In conclusion, this approach can be implemented to deliver transgene expression, to study gene function and to conduct pre-clinical therapeutic target validation in the spinal cord.

Supplementary Material

Refer to Web version on PubMed Central for supplementary material.

Acknowledgments

We thank Dr. Hongyan Wang for advice and Ms Karen Tran for editing the manuscript. This work was supported by grants from The ALS Association to Z.X.; from Jacob's Cure, NTSAD Foundation, and Canavan Foundation and National Institutes of Health R01 grant (1R01NS076991) to G.G., and partially supported by a grant from National High Technology Research and Development Program (“863” Program) of China (2012AA020810) to G.G.; and from China scholarship council and Chinese society of neurology to Y.G.

References

1. Ray MK, Fagan SP, Brunicardi FC. The Cre-loxP system: a versatile tool for targeting genes in a cell- and stage-specific manner. Cell Transplant. 2000; 9(6):805–815. [PubMed: 11202567]
2. Zinn E, Vandenberghe LH. Adeno-associated virus: fit to serve. Current Opinion in Virology. 2014; 8(0):90–97. [PubMed: 25128609]
3. Snyder BR, Gray SJ, Quach ET, Huang JW, Leung CH, Samulski RJ, Boulis NM, Federici T. Comparison of adeno-associated viral vector serotypes for spinal cord and motor neuron gene delivery. Hum Gene Ther. 2011; 22(9):1129–1135. [PubMed: 21443428]
4. Federici T, Taub JS, Baum GR, Gray SJ, Grieger JC, Matthews KA, Handy CR, Passini MA, Samulski RJ, Boulis NM. Robust spinal motor neuron transduction following intrathecal delivery of AAV9 in pigs. Gene Ther. 2012; 19(8):852–859. [PubMed: 21918551]
5. Bevan AK, Duque S, Foust KD, Morales PR, Braun L, Schmelzer L, Chan CM, McCrate M, Chicoine LG, Coley BD, Porensky PN, Kolb SJ, Mendell JR, Burghes AH, Kaspar BK. Systemic gene delivery in large species for targeting spinal cord, brain, and peripheral tissues for pediatric disorders. Mol Ther. 2011; 19(11):1971–1980. DOI: 10.1038/mt.2011.157 [PubMed: 21811247]

6. Samaranch L, Salegio EA, San Sebastian W, Kells AP, Foust KD, Bringas JR, Lamarre C, Forsayeth J, Kaspar BK, Bankiewicz KS. Adeno-associated virus serotype 9 transduction in the central nervous system of nonhuman primates. Hum Gene Ther. 2012; 23(4):382–389. [PubMed: 22201473]
7. Gray SJ, Nagabhushan Kalburgi S, McCown TJ, Jude Samulski R. Global CNS gene delivery and evasion of anti-AAV-neutralizing antibodies by intrathecal AAV administration in non-human primates. Gene Ther. 2013; 20:450–459. [PubMed: 23303281]
8. Wang H, Yang B, Qiu L, Yang C, Kramer J, Su Q, Guo Y, Brown RH Jr, Gao G, Xu Z. Widespread spinal cord transduction by intrathecal injection of rAAV delivers efficacious RNAi therapy for amyotrophic lateral sclerosis. Hum Mol Genet. 2014; 23(3):668–681. [PubMed: 24108104]
9. Hordeaux J, Dubreil L, Deniaud J, Iacobelli F, Moreau S, Ledevin M, Le Guiner C, Blouin V, Le Duff J, Mendes-Madeira A, Rolling F, Cherel Y, Moullier P, Colle MA. Efficient central nervous system AAVrh10-mediated intrathecal gene transfer in adult and neonate rats. Gene Ther. 2015
10. Schuster DJ, Dykstra JA, Riedl MS, Kitto KF, Belur LR, McIvor RS, Elde RP, Fairbanks CA, Vulchanova L. Biodistribution of adeno-associated virus serotype 9 (AAV9) vector after intrathecal and intravenous delivery in mouse. Front Neuroanat. 2014; 8:42. [PubMed: 24959122]
11. Zhang H, Yang B, Mu X, Ahmed SS, Su Q, He R, Wang H, Mueller C, Sena-Esteves M, Brown R, Xu Z, Gao G. Several rAAV vectors efficiently cross the blood-brain barrier and transduce neurons and astrocytes in the neonatal mouse central nervous system. Mol Ther. 2011; 19(8):1440–1448. DOI: 10.1038/mt.2011.98 [PubMed: 21610699]
12. Fairbanks CA. Spinal delivery of analgesics in experimental models of pain and analgesia. Adv Drug Deliv Rev. 2003; 55(8):1007–1041. [PubMed: 12935942]
13. Ciesielska A, Hadaczek P, Mittermeyer G, Zhou S, Wright JF, Bankiewicz KS, Forsayeth J. Cerebral infusion of AAV9 vector-encoding non-self proteins can elicit cell-mediated immune responses. Mol Ther. 2013; 21(1):158–166. [PubMed: 22929660]
14. Klein RL, Dayton RD, Leidenheimer NJ, Jansen K, Golde TE, Zweig RM. Efficient neuronal gene transfer with AAV8 leads to neurotoxic levels of tau or green fluorescent proteins. Mol Ther. 2006; 13(3):517–527. [PubMed: 16325474]
15. Rennels ML, Gregory TF, Blaumanis OR, Fujimoto K, Grady PA. Evidence for a ‘paravascular’ fluid circulation in the mammalian central nervous system, provided by the rapid distribution of tracer protein throughout the brain from the subarachnoid space. Brain Res. 1985; 326(1):47–63. [PubMed: 3971148]
16. Iliff JJ, Wang M, Liao Y, Plogg BA, Peng W, Gundersen GA, Benveniste H, Vates GE, Deane R, Goldman SA, Nagelhus EA, Nedergaard M. A paravascular pathway facilitates CSF flow through the brain parenchyma and the clearance of interstitial solutes, including amyloid beta. Sci Transl Med. 2012; 4(147):147ra111.
17. Duque S, Joussemet B, Riviere C, Marais T, Dubreil L, Douar AM, Fyfe J, Moullier P, Colle MA, Barkats M. Intravenous administration of self-complementary AAV9 enables transgene delivery to adult motor neurons. Mol Ther. 2009; 17(7):1187–1196. DOI: 10.1038/mt.2009.71 [PubMed: 19367261]
18. Foust KD, Nurre E, Montgomery CL, Hernandez A, Chan CM, Kaspar BK. Intravascular AAV9 preferentially targets neonatal neurons and adult astrocytes. Nat Biotechnol. 2009; 27(1):59–65. DOI: 10.1038/nbt.1515 [PubMed: 19098898]
19. Yang B, Li S, Wang H, Guo Y, Gessler DJ, Cao C, Su Q, Kramer J, Zhong L, Ahmed SS, Zhang H, He R, Desrosiers RC, Brown R, Xu Z, Gao G. Global CNS Transduction of Adult Mice by Intravenously Delivered rAAVrh.8 and rAAVrh.10 and Nonhuman Primates by rAAVrh.10. Mol Ther. 2014; 22(7):1299–1309. [PubMed: 24781136]
20. Rennels ML, Blaumanis OR, Grady PA. Rapid solute transport throughout the brain via paravascular fluid pathways. Adv Neurol. 1990; 52:431–439. [PubMed: 2396537]
21. Aird RB. A study of intrathecal, cerebrospinal fluid-to-brain exchange. Exp Neurol. 1984; 86(2): 342–358. [PubMed: 6548450]
22. Crawley JN, Fiske SM, Durieux C, Derrien M, Roques BP. Centrally administered cholecystokinin suppresses feeding through a peripheral-type receptor mechanism. J Pharmacol Exp Ther. 1991; 257(3):1076–1080. [PubMed: 2046021]

23. Bozanovic-Sosic R, Mollanji R, Johnston MG. Spinal and cranial contributions to total cerebrospinal fluid transport. Am J Physiol Regul Integr Comp Physiol. 2001; 281(3):R909–916. [PubMed: 11507008]

24. Johnston M, Papaiconomou C. Cerebrospinal fluid transport: a lymphatic perspective. News Physiol Sci. 2002; 17:227–230. [PubMed: 12433975]

25. Pollay M. The function and structure of the cerebrospinal fluid outflow system. Cerebrospinal Fluid Res. 2010; 7:9. [PubMed: 20565964]

26. Nonnenmacher M, Weber T. Intracellular transport of recombinant adeno-associated virus vectors. Gene Ther. 2012; 19(6):649–658. [PubMed: 22357511]

27. Liu B, Paton JF, Kasparov S. Viral vectors based on bidirectional cell-specific mammalian promoters and transcriptional amplification strategy for use in vitro and in vivo. BMC Biotechnol. 2008; 8:49. [PubMed: 18485188]

28. von Jonquieres G, Mersmann N, Klugmann CB, Harasta AE, Lutz B, Teahan O, Housley GD, Frohlich D, Kramer-Albers EM, Klugmann M. Glial promoter selectivity following AAV-delivery to the immature brain. PLoS One. 2013; 8(6):e65646. [PubMed: 23799030]

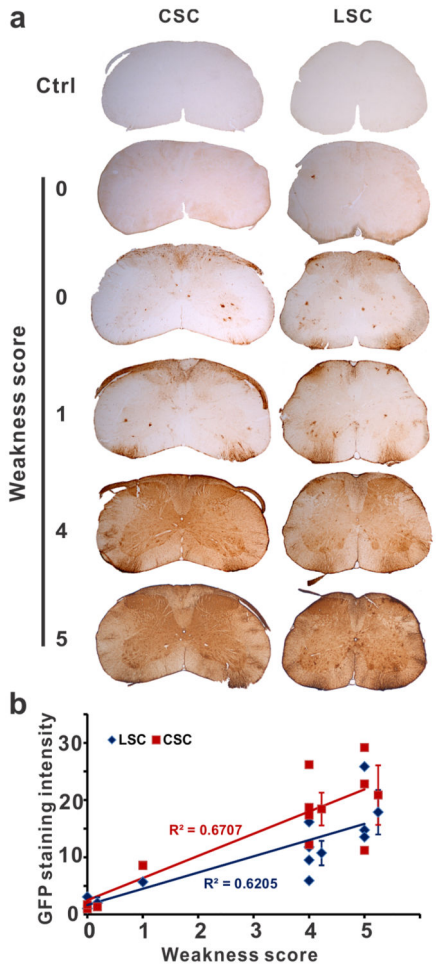

Fig. 1.

Lidocaine-induced weakness score predicted the transduction efficiency. (a) rAAV together with 1% lidocaine in PBS were injected by lumbar puncture. The injection quality was scored based on the degree of lidocaine-induced transient weakness. Zero indicates no weakness and five indicates the severest weakness (see Methods). Three weeks later the mice were sacrificed and examined for GFP expression by immunohistochemistry. Representative staining from cervical (CSC) and lumbar spinal cord (LSC) sections of the injected mice and the uninjected controls (Ctrl) are shown. (b) The GFP staining intensity in both lumbar and cervical spinal cord was directly correlated with the degree of weakness immediately after the injection. Each mark represents values from one mouse. Marks with error bars (standard deviation) represent average of four mice scored at 4 and three mice scored at 5.

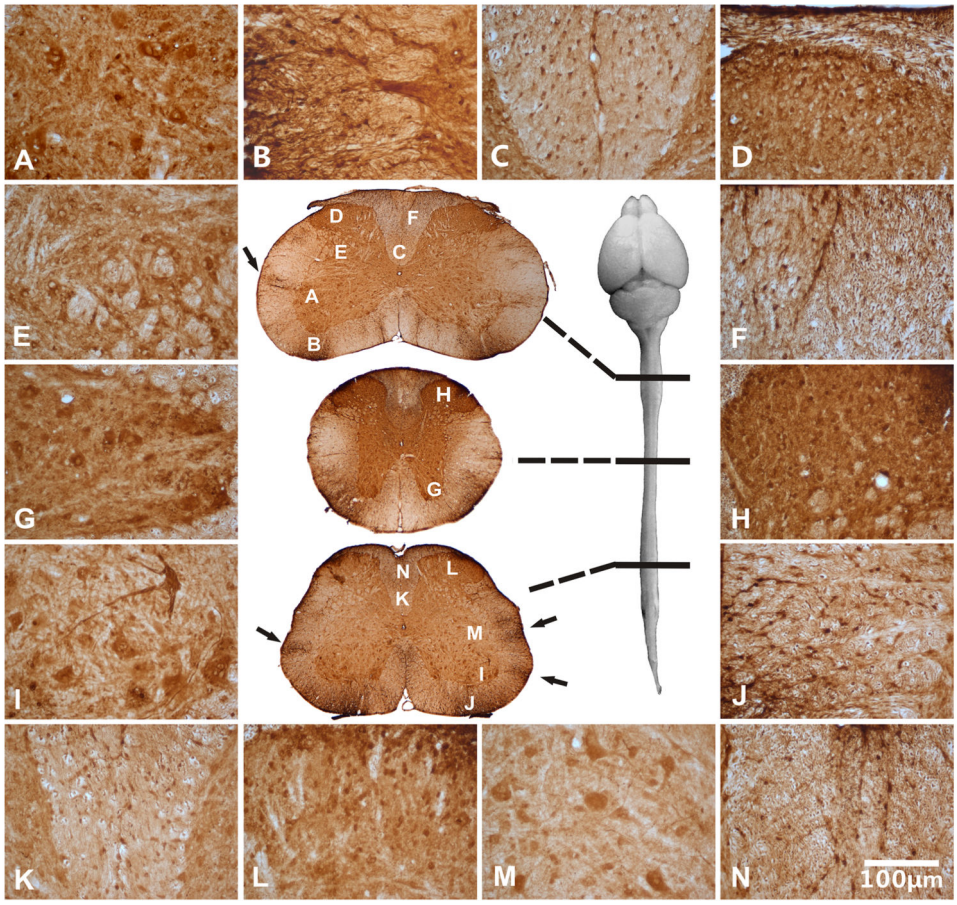

Fig. 2.

rAAVrh10 injected into the lumbar cistern transduced cells in lumbar, thoracic, and cervical spinal cord (Central panel). Areas of the cervical (A-F), thoracic (G-H) and lumbar spinal cord (I-N) were viewed in high magnification: (A) ventral horn, (B) ventral root exit zone, (C) corticospinal tract, (D) dorsal horn, (E) intermediate horn, (F) dorsal funiculus, (G) ventral horn, (H) dorsal horn, (I) ventral horn, (J) ventral root exit zone, (K) corticospinal tract, (L) dorsal horn, (M) intermediate horn and (N) dorsal funiculus. All peripheral panels are in the same magnification. Arrows in the central panel point to patches of transduction that appeared to project from the edge into the parenchyma of the spinal cord (see text). Bar=100μm.

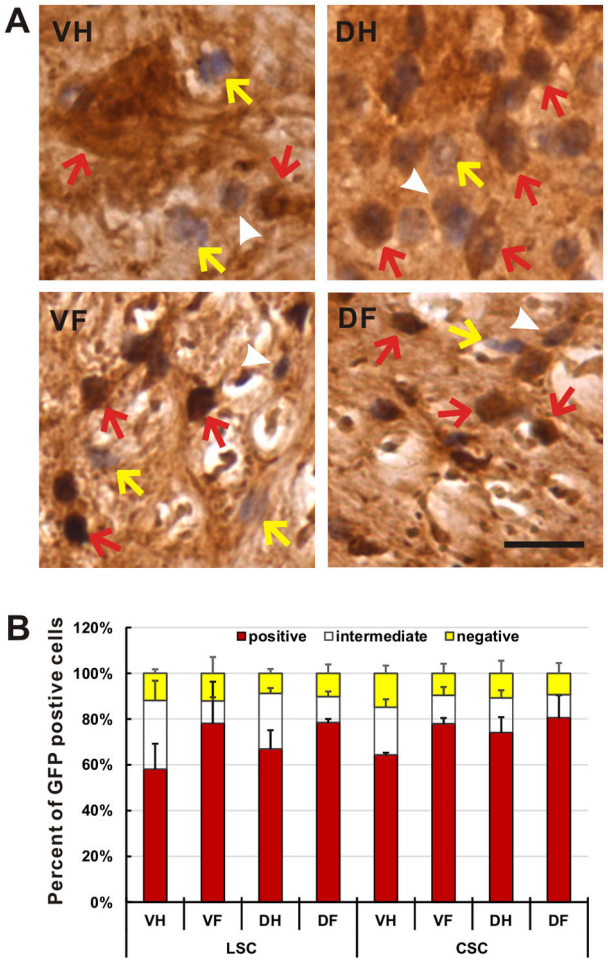

Fig. 3.

rAAVrh10 injected into the lumbar cistern transduced cells in the spinal cord with a high efficiency. (a) Spinal cord sections from animals with injection scores at 4 or 5 were immunostained with GFP antibody were counterstained with haematoxylin. The transduced and untransduced cells were counted and categorized into three groups: transduced (GFP-positive with dark brown signal, red arrows), possibly transduced (possible GFP-positive with light brown signal, white arrowheads) and untransduced (GFP-negative with no brown signal, yellow arrows). Bar = 30μm. (b) Approximately 60-90% of the cells were transduced in four representative areas of the lumbar and the cervical spinal cords. Bars represent the average of three animals. Yellow bars represent the fraction of GFP-negative cells (yellow arrows in a). White bars represent the fraction of possible GFP-positive cells (white arrowheads in a). Red bars represent the fraction of GFP-positive cells (red arrows in a). Error bars are standard deviation. VH = ventral horn, DH = dorsal horn, VF = ventral funiculus, DF = dorsal funiculus.

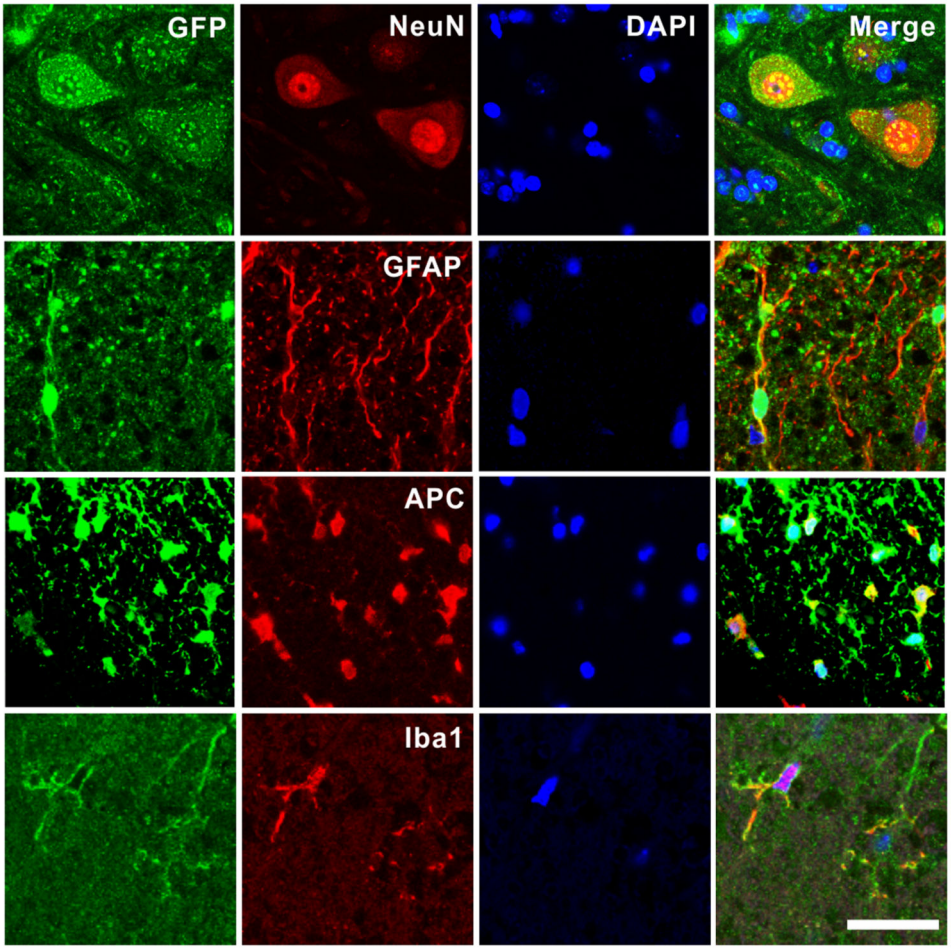

Fig. 4.

rAAVrh10 injected into the lumbar cistern transduced neurons, astrocytes, oligodendrocytes and microglia in the spinal cord. Spinal cord sections were doubly stained for GFP and various cell markers: NeuN for neurons, GFAP for astrocytes, APC for oligodenrocytes and Iba1 for microglia. Notice the robust GFP signal in motor neurons in the panels of the top row. Bar = 50μm.

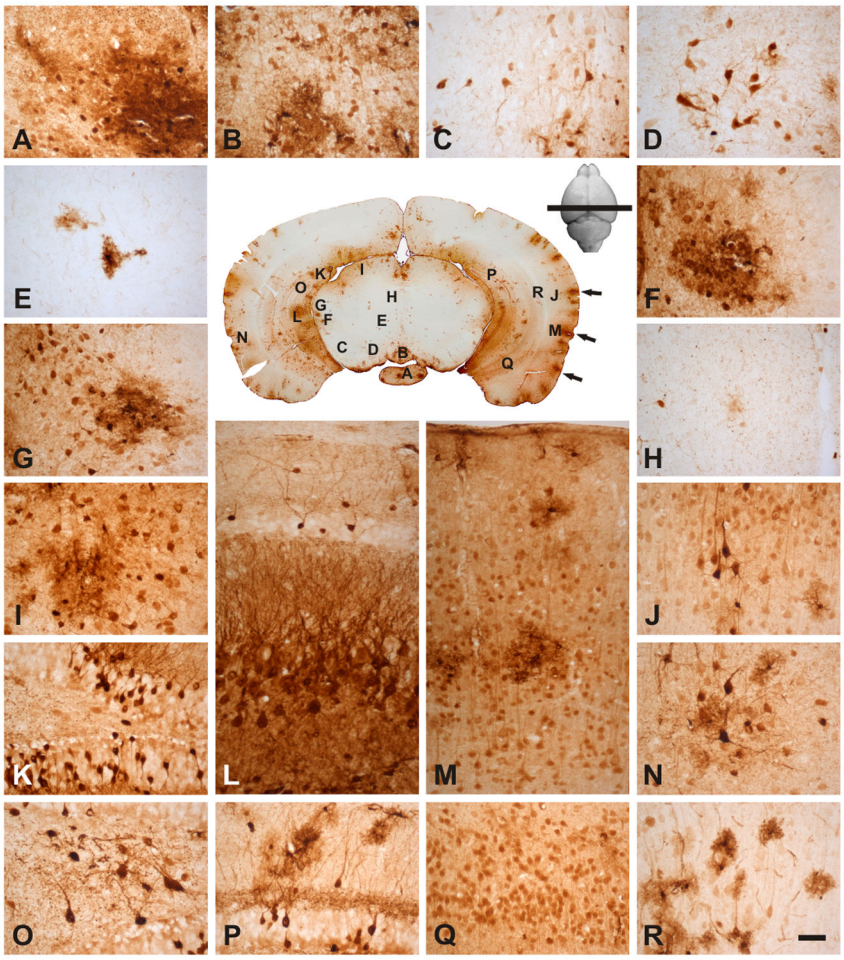

Fig. 5.

rAAVrh10 injected into the lumbar cistern transduced regions in the cortex, hippocampus and rostral midbrain: (A) medial mammillary nucleus, (B) rostral interpeduncular nucleus. (C) substantia nigra, (D) parabrachial pigmented nucleus, (E) red nucleus, (F) posterior intralaminar thalamic nucleus, (G) medial geniculate nucleus, (H) periaqueductal gray, (I) superior colliculus, (K, O, P) dentate gyrus, (L, Q) CA3 of the hippocampus, (J, M, N, R) cortex. Note that the temporal cortex had higher level of transduction compared with the parietal cortex; in hippocampus, the most prominent level of transduction was found in dentate gyrus and CA3; in the midbrain, most transduction was in the peripheral regions. Arrows in the central panel point to patches of transduction that appeared to project from the edge into the parenchyma of the brain (see text). Bar = 50μm.

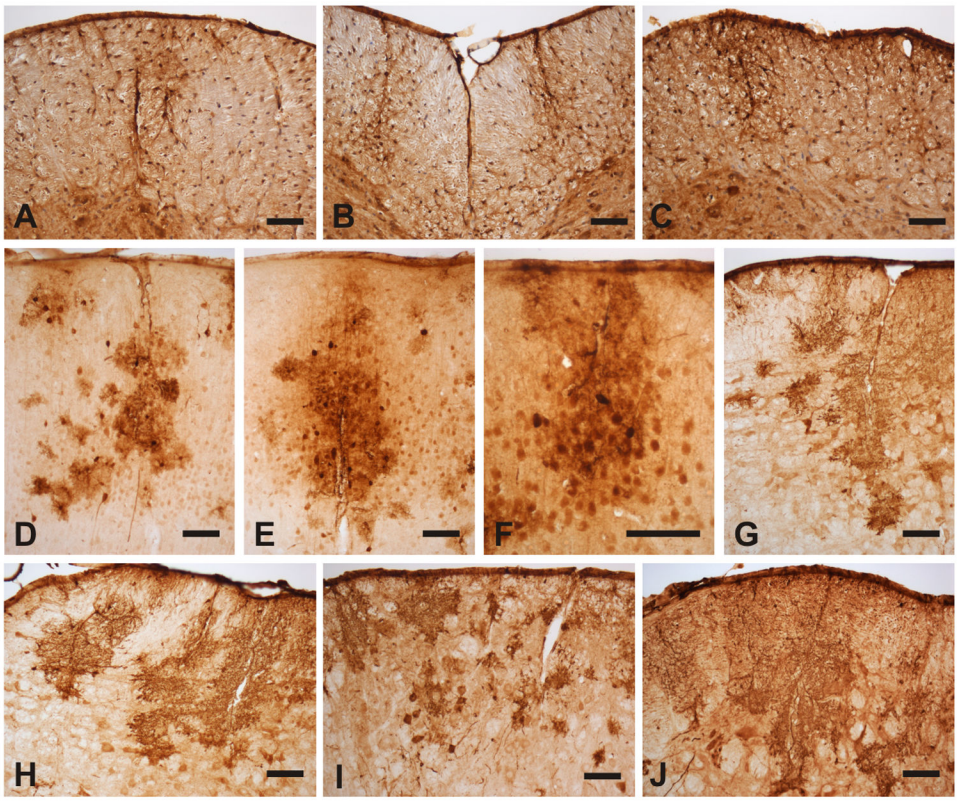

Fig. 6.

The rAAV transduction was distributed as long patches projecting from the surface into the parenchyma of the spinal cord and the cortex: (A) lateral and (B) anterior funiculi of the CSC, (C) lateral funiculus of the LSC, (D) frontal cortex, (E) parietal cortex, (F) temporal cortex, (G, H) ventral medial part of Pons, (I) ventral anterior part of Pons, (J) ventral lateral part of Pons. Bar = 100 μm.

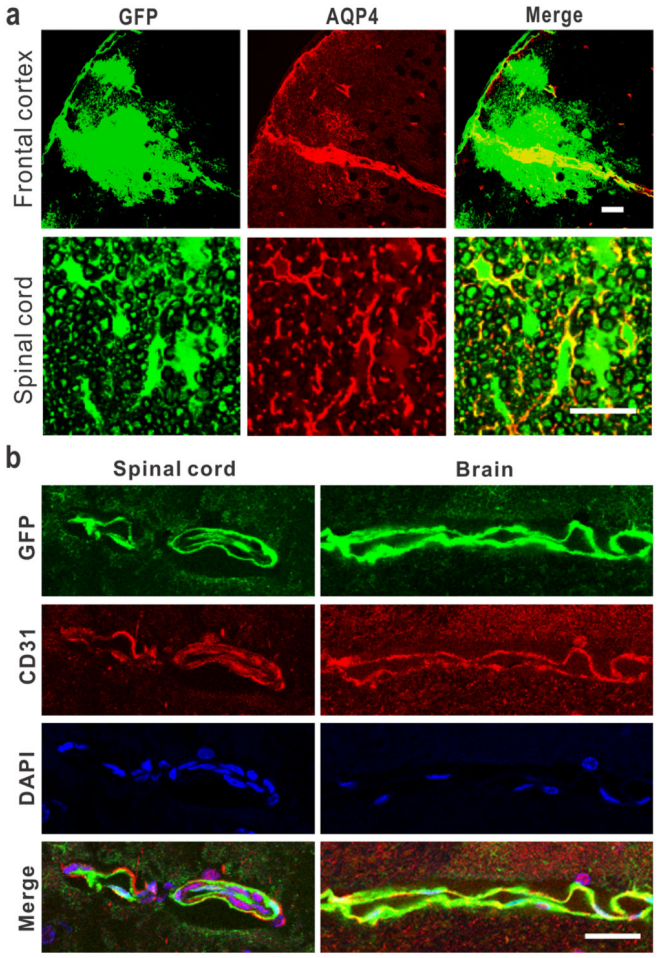

Fig. 7.

rAAV penetrates into the CNS parenchyma through the perivascular spaces of Virchow-Robin. (a) Doublefluorescence staining showing colocalization of perivascular space (AQP-4) with GFP signal in the cortex and the spinal cord. Bar = 30 μm in the cortex, 100 μm in the spinal cord. (b) Doublefluorescence staining showing the rAAV transduction in the endothelial cells (CD31) in the spinal cord and brain. Bar = 30 μm.

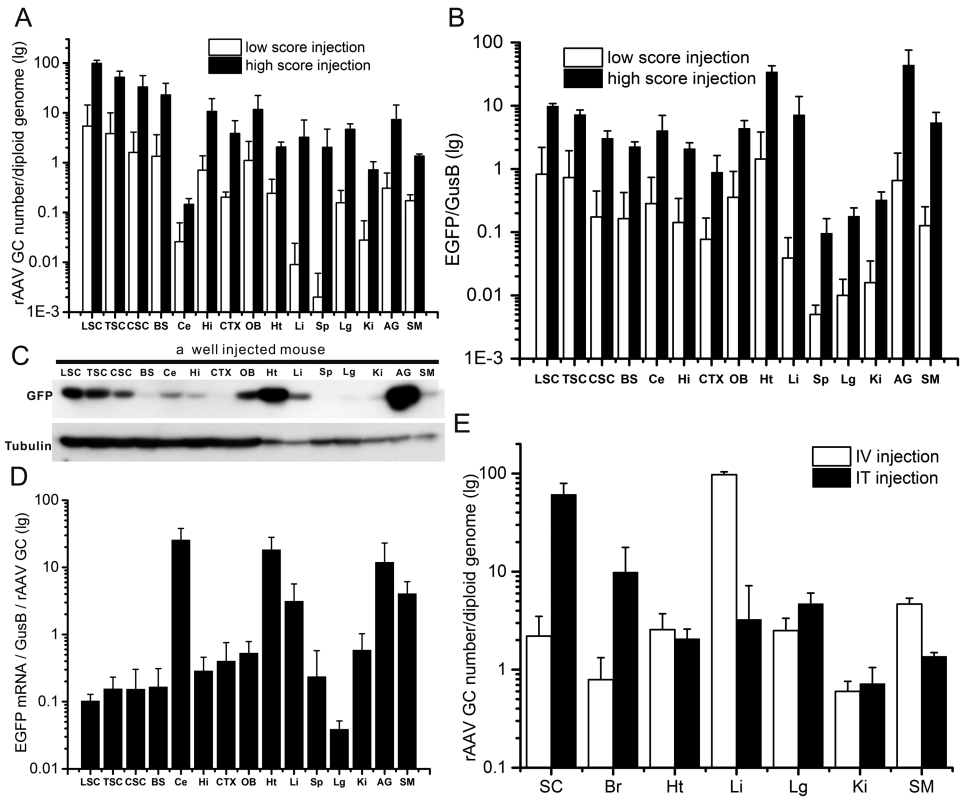

Fig. 8.

rAAV distribution and transgene expression after its injection into the lumbar cistern. (a) Quantification of rAAV genome copies in regions of the CNS and the periphery. White bars represent the levels from the poorly injected animals with low weakness score. Black bars represent the levels from the well injected animals with high weakness score. (b) Quantification of the GFP mRNA. White and black bars represent the same as in A. (c) Western blot for GFP expression. Tubulin was probed as loading control. (d) EGFP expression normalized by rAAV genome copy in regions of the CNS and the periphery in well injected mice. (e) Comparison of the rAAVrh10 genome copies in regions of the CNS and the periphery between the mice injected intravenously (IV) [19] and those injected intrathecally (IT). LSC = lumbar spinal cord, TSC = thoracic spinal cord, CSC = cervical spinal cord, BS = brainstem, Ce = cerebellum, Hi = hippocampus, CTX = cortex, OB = olfactory bulb, Ht = heart, Li = liver, Sp = spleen, Lg = lung, Ki = kidney, AG = adrenal gland, SM = skeletal muscle, Br = brain. All error bars are standard deviation.